applied sciences

Article

Effect of Moulding Moisture Content on the Mechanical Behaviour of Unsaturated Rockfill Material

Gengyao Cui [1], Huizong Yan [2], Degao Zou [1], Fanwei Ning [1,*], Jingmao Liu [1], Chenguang Zhou [1] and Xinyuan Zhang [2]

[1] The State Key Laboratory of Coastal and Offshore Engineering, Dalian University of Technology, Dalian 116024, China; cuigengyao@mail.dlut.edu.cn (G.C.); zoudegao@dlut.edu.cn (D.Z.); liujm@dlut.edu.cn (J.L.); zhchg@dlut.edu.cn (C.Z.)
[2] POWERCHINA Kunming Engineering Corporation, Limited, No. 115, East Renmin Road, Kunming 652501, China
* Correspondence: ningfw@dlut.edu.cn

Abstract

In rockfill dams and high-fill engineering projects, rockfill materials are compacted under different moisture conditions and remain unsaturated during construction and service, yet the influence of the moulding moisture content on their subsequent mechanical behaviour has not been systematically clarified. In particular, it remains unclear whether the observed moisture-dependent response results only from the moisture condition. To address this issue, large-scale consolidated-drained triaxial tests were conducted on unsaturated rockfill specimens with different moulding moisture contents ranging from 0% to 3%, initial porosities of 19% and 21%, and fines contents (the content of particles smaller than 5 mm) of 19% and 35%. The results show that increasing the moulding moisture content reduced peak deviatoric stress, while the final strength weakening coefficient stabilised within 0.87–0.91. In contrast, the initial modulus first decreased and then recovered, and may even have exceeded that of the dry specimen. Higher moisture contents suppressed dilation under low confining pressures and promoted particle breakage and volumetric compression under high confining pressures, with both the content of particles smaller than 5 mm and the peak volumetric compression increasing markedly. The moisture content effect also depended on the initial density and fines content. Specimens with lower fines contents were more sensitive to moisture variation, whereas higher porosity weakened this effect. Distinct mechanical responses persisted after saturation, indicating that the moulding moisture content acts not only through suction during shearing but also through particle rearrangement and contact states formed during compaction. Therefore, moulding moisture content should be regarded as an important parameter in field construction and laboratory testing.

Keywords: moulding moisture content; shear strength; large-scale triaxial test; unsaturated rockfill; initial stiffness

Check for updates

Received: 1 September 2026
Revised: 12 September 2026
Accepted: 16 September 2026
Published: 18 September 2026

Copyright: © 2026 by the authors. Licensee MDPI, Basel, Switzerland. This article is an open access article distributed under the terms and conditions of the Creative Commons Attribution (CC BY) license.

1. Introduction

Coarse-grained soils, such as rockfill materials and gravelly soils, are widely used as major fill materials in large geotechnical projects, including earth-rock dams, airports, and high-fill subgrades [1–6]. During construction, these materials are commonly spread in layers and compacted at a specified moisture content to reach the target dry density. They then remain unsaturated during construction, before reservoir impoundment, and during long-term operation [7,8]. Early deformation of the fill body is closely related to project stability and long-term safety and is largely governed by the stiffness and shear strength of the compacted rockfill [1,2,9,10]. However, even when the dry density satisfies the design requirement, the moisture content of the fill may still vary considerably. Such variations may alter interparticle contacts and affect the deformation and long-term performance of the fill body. Previous studies have shown that moisture content and fines content jointly affect the strength and permanent deformation of coarse–fine mixtures [11–14]. Therefore, a systematic investigation of the macroscopic mechanical properties of compacted unsaturated rockfill materials and their dependence on moisture content is essential for optimising construction compaction control, thereby supporting the safe and sustainable development of hydropower projects.

It is well established that the stress–strain relationship, dilatancy, and peak strength of rockfill materials are jointly controlled by confining pressure, porosity, gradation, particle shape, and particle breakage [1,2,15–18]. Moisture also significantly affects the mechanical behaviour of coarse-grained soils. Oldecop and Alonso [7] showed through one-dimensional compression tests that relative humidity affects crack propagation and particle breakage, with collapse deformation at 100% relative humidity approaching that of saturated specimens. Mao et al. [19] found that increasing humidity reduces peak shear strength, increases contraction, and enhances particle breakage in soft-rock coarse-grained materials. These findings are consistent with studies showing that wetting-induced deformation is closely related to the degradation of particle strength [20,21]. From the perspective of unsaturated soil mechanics, increasing water content generally reduces matric suction and consequently decreases stiffness and shear strength [22–25]. Most existing studies, therefore, treat moisture as a factor that promotes material softening and structural degradation and explain the hydro-mechanical response of coarse-grained soils from the perspectives of suction reduction, moisture-induced softening, and particle breakage.

However, the effect of moulding moisture content is not limited to the suction state during testing or moisture-induced weakening associated with wetting. Previous studies have shown that different moulding water contents produce distinct initial fabrics, which subsequently affect compression, shearing, small-strain stiffness, and volumetric behaviour [26–28]. Using scanning electron microscopy and mercury intrusion porosimetry, Delage et al. [29] showed that specimens compacted dry of optimum, at optimum, and wet of optimum developed different particle skeletons and pore-size distributions. Magistris [30] found that even after the effect of dry density was accounted for, moulding water content still exerted a marked influence on small-strain stiffness. Specimens compacted at the optimum water content exhibited the lowest isotropic compressibility and the highest initial stiffness. Zhang et al. [31] similarly reported a non-monotonic variation in the maximum shear modulus among specimens compacted to the same dry density but at different water contents. More recently, Ng and Peprah-Manu [32] and Dai et al. [33] have further shown that moulding water content and dry density influence the hydromechanical response of compacted soils by altering their pore structure, structural characteristics, and stiffness anisotropy. Compared with fine-grained soils, coarse-grained soils such as rockfill and gravelly soils have more pronounced skeleton contacts, multi-scale pores, and higher breakage sensitivity. Existing studies have mostly focused on the softening behaviour of rockfill after saturation or wetting deformation during loading. The influence of moulding moisture content on initial fabric, early shear stiffness, and macroscopic mechanical response remains insufficiently understood.

To address these issues, this study used rockfill material from an actual dam project and conducted a series of large-scale triaxial shear tests on unsaturated rockfill specimens. The effects of moulding moisture content on the stress–strain relationship, peak strength, and initial modulus of the unsaturated rockfill were systematically investigated. By comparing the mechanical responses under different test conditions, the variation in the moulding moisture content effect with different fines contents and porosities was further analysed. The results provide an experimental basis for controlling compaction moisture content and predicting early-stage deformation in large coarse-grained soil filling projects.

2. Materials and Testing Procedures

2.1. Test Material and Apparatus

The tested material was obtained from the main rockfill zone of a gravelly soil core-wall dam project in Sichuan Province, Southwestern China. The parent rock was slate. Typical particles are shown in Figure 1a. The particles were generally platy and angular, representing the typical morphology of blasted rockfill materials. The specific gravity of the rock particles was 2.71. The average uniaxial compressive strengths of the parent rock under dry and wet conditions were 88.6 MPa and 68.5 MPa [34], respectively, and the softening coefficient was 0.77. To further characterise the mineral composition of the material, X-ray diffraction analysis was performed on parent rock samples, as shown in Figure 1b. The results indicate that the rockfill mainly consisted of hard silicate minerals, including quartz (48.1%), albite (13.0%), calcite (1.8%), muscovite (28.7%), and a small proportion of the clay mineral clinochlore (8.4%). The detailed properties of the material are summarised in Table 1.

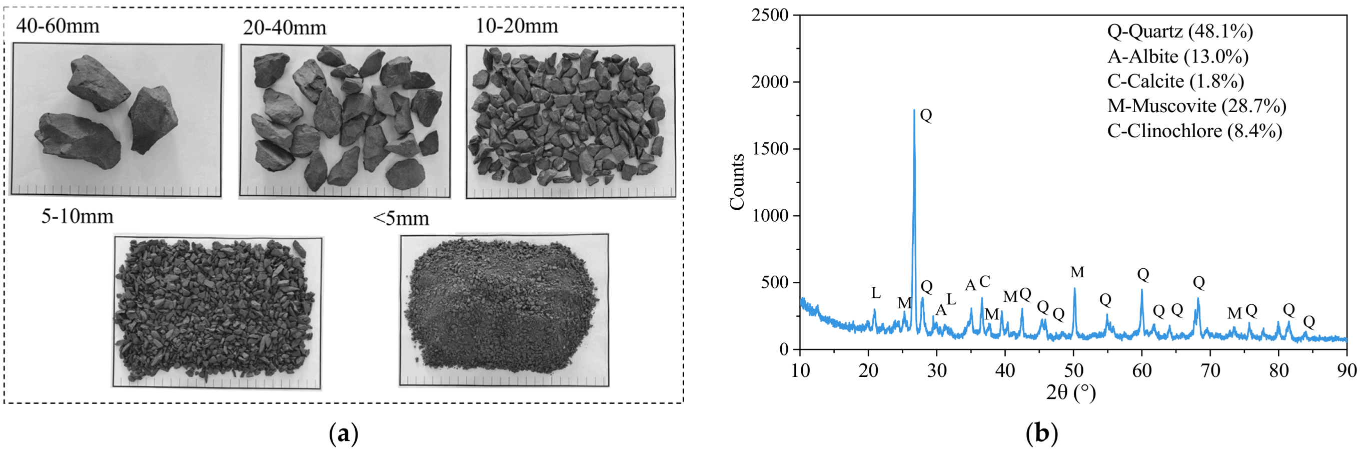

Figure 1. Tested rockfill material: (**a**) typical particles; (**b**) mineralogical composition obtained by X-ray diffraction.

Table 1. Properties of the tested material.

Properties of Rockfill Material	Value
Physical and mechanical properties	
Specific gravity G_s	2.71
Uniaxial compressive strength of parent rock under dry conditions (MPa)	88.6
Uniaxial compressive strength of parent rock under saturated conditions (MPa)	68.5
Softening coefficient	0.77
Mineral content of the sample	
Quartz (%)	48.1
Albite (%)	13.0
Calcite (%)	1.8
Muscovite (%)	28.7
Clinochlore (%)	8.4

Large-scale consolidated-drained triaxial shear tests on unsaturated rockfill specimens were conducted using a large-scale high-pressure triaxial apparatus, as shown in Figure 2. The apparatus could accommodate specimens up to 300 mm in diameter and 700 mm in height. It consisted mainly of an axial servo loading system, a pressure chamber, a confining-pressure servo system, a data acquisition and control system, and a volumetric deformation measurement system. Because the specimens remained unsaturated during shearing, the conventional drainage-based volume change measurement method could not be used to directly obtain the specimen volume change. To measure the volume change of unsaturated specimens during testing, an additional lateral displacement sensor was installed in the confining-pressure system. The actual specimen volume change was back-calculated from the monitored water volume change in the entire system. This method can continuously record the volumetric deformation of unsaturated rockfill specimens during consolidation and shearing and is suitable for large-scale triaxial tests on unsaturated coarse-grained soils. Its reliability has been verified in previous studies [20,21].

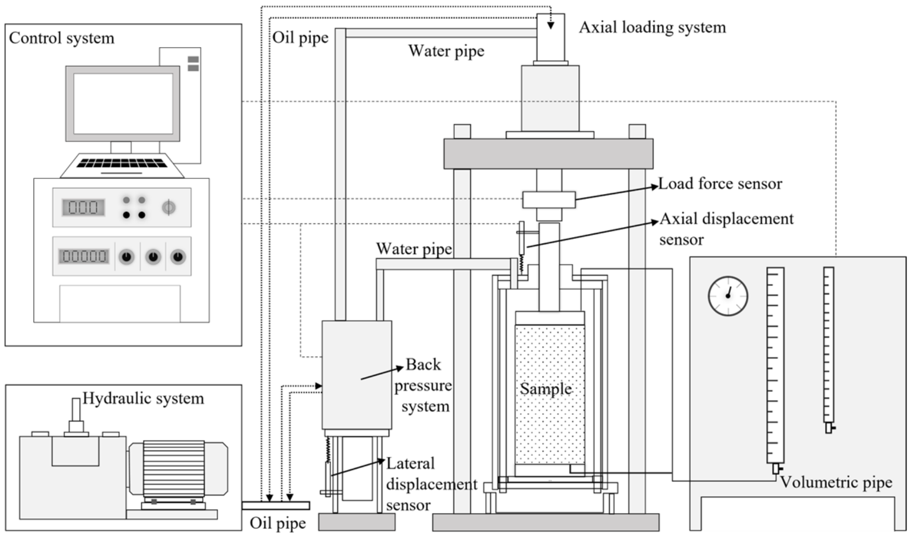

Figure 2. Triaxial apparatus.

2.2. Testing Programme and Procedures

The maximum particle size of the field prototype rockfill was much larger than that permitted in large-scale laboratory triaxial specimens. Therefore, the prototype gradation could not be used directly in the laboratory triaxial tests. To ensure the representativeness of the test results and satisfy the required ratio between specimen diameter and maximum particle size, the field prototype gradation was scaled down. According to the requirement that the ratio of specimen diameter to maximum particle size should not be less than 5 in large-scale triaxial tests on coarse-grained soils, the maximum particle size in this study was set at 60 mm [35]. Two scaled gradations were then obtained using the parallel technique and the replacement technique, denoted as Gradation A and Gradation B, respectively, as shown in Figure 3. Gradation A was used as the reference gradation to systematically examine the effect of the moulding moisture content on the mechanical behaviour of unsaturated rockfill. Gradation B was used mainly to compare the influence of the fines content on the moulding moisture content effect. The contents of particles finer than 5 mm ($P_{<5\text{mm}}$) in the two corresponding gradations were 35% and 19%, respectively. The porosity n was set at 19%, which corresponds to the average porosity of the field-compacted fill.

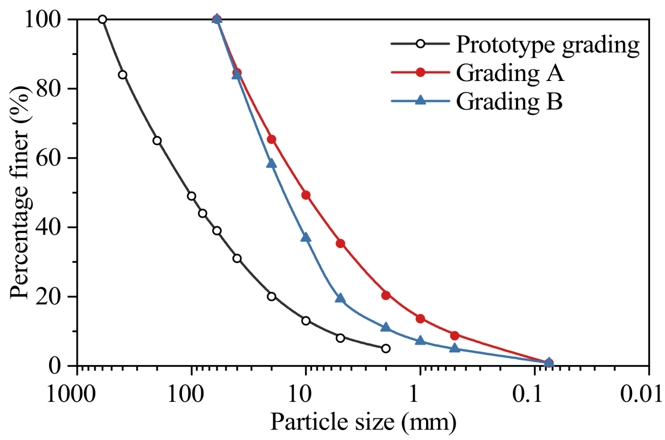

Figure 3. Particle size distribution of the tested rockfill material.

Laboratory compaction tests for determining the maximum dry density ρ_{dmax} were first conducted according to the relevant standard using the vibratory compaction method [35]. The results are shown in Figure 4. Figure 5 shows typical photographs of the rockfill material after uniform mixing at different moisture contents. The dry density first decreased and then increased with increasing moisture content. This trend is consistent with the laboratory dry-density results for high-speed railway graded aggregate materials [36]. Considering that the measured moisture content of the field fill fell mainly within the range of 0–3%, this range was adopted for unsaturated static shear tests on rockfill specimens with two different gradations. In addition, a low-density group was prepared to examine the influence of porosity on the moulding moisture content effect. The specific test conditions are listed in Table 2.

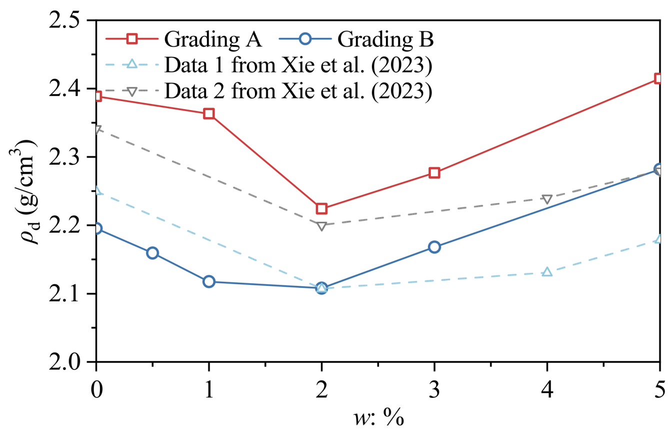

Figure 4. Effect of moisture content on the maximum dry density [36].

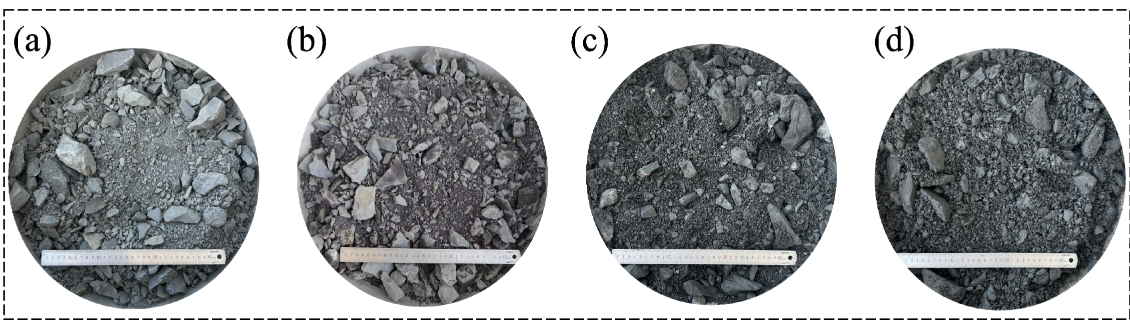

Figure 5. Typical photographs of rockfill material after uniform mixing at different moulding moisture contents: (**a**) w = 0%, (**b**) w = 1%, (**c**) w = 2% and (**d**) w = 3%.

Table 2. Test conditions.

PSD	σ_3 (MPa)	w (%)	n (%)
Gradation A	0.2, 0.6, 1.2, 2.5	0, 1, 2, 3	19
	0.6	0, 1, 2, 3	21
Gradation B	0.6	0, 0.5, 1, 2	19

Before testing, the raw material was air-dried and sieved. The required mass of each particle-size group was calculated according to the target gradation, particle specific gravity, and porosity, and the groups were then fully mixed. For specimens prepared with added water, the amount of water was calculated from the dry mass and target moisture content. Water was added by uniform spraying and continuous mixing. The mixed material was sealed and stored for at least 24 h to allow water to migrate among particles of different sizes and become uniform. The tests were conducted in accordance with the relevant ASTM [37]. During specimen preparation, the layered undercompaction method and vibratory compaction were used to ensure uniform density along the specimen height. The specimens had a diameter of 300 mm and a height of 700 mm. A photograph of a typical specimen is shown in Figure 6. After preparation, the top cap was installed, the rubber membrane was sealed, and the specimen was placed in the triaxial pressure chamber for water injection and airtightness checking. The confining pressure was then increased stepwise to the target value for isotropic consolidation. Shearing started after the axial deformation and volumetric deformation became stable. During shearing, axial loading was applied under displacement control at a constant strain rate of 0.1%/min. Axial load, axial displacement, confining pressure, and water volume change in the pressure chamber were recorded simultaneously. After testing, the specimen was oven-dried and sieved to obtain the post-shearing particle size distribution.

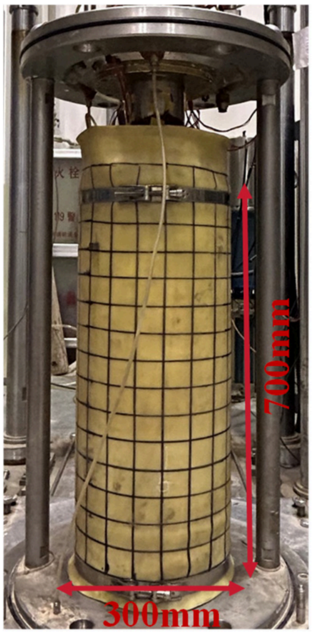

Figure 6. Photograph of typical sample.

2.3. Experimental Repeatability and Moisture Content Determination

To verify the reliability of the triaxial test results for unsaturated rockfill, repeatability tests were performed at the same initial moulding moisture content, as shown in Figure 7. Under the same moisture condition, the deviatoric stress–axial strain curves and volumetric strain–axial strain curves of duplicate specimens show consistent magnitudes and evolution trends, indicating good repeatability. In addition, to further confirm the moisture content control during testing, the final moisture content, w_{end}, was measured after each test. For specimens with a target moisture content of 1%, the measured final moisture contents were 0.92% and 1.01%. For specimens with a target moisture content of 2%, the measured values were 1.89% and 1.94%. These small differences confirm that no obvious water evaporation or external water intrusion occurred during specimen preparation or throughout the test. The high repeatability and accurate moisture control provide a reliable experimental basis for the subsequent analysis.

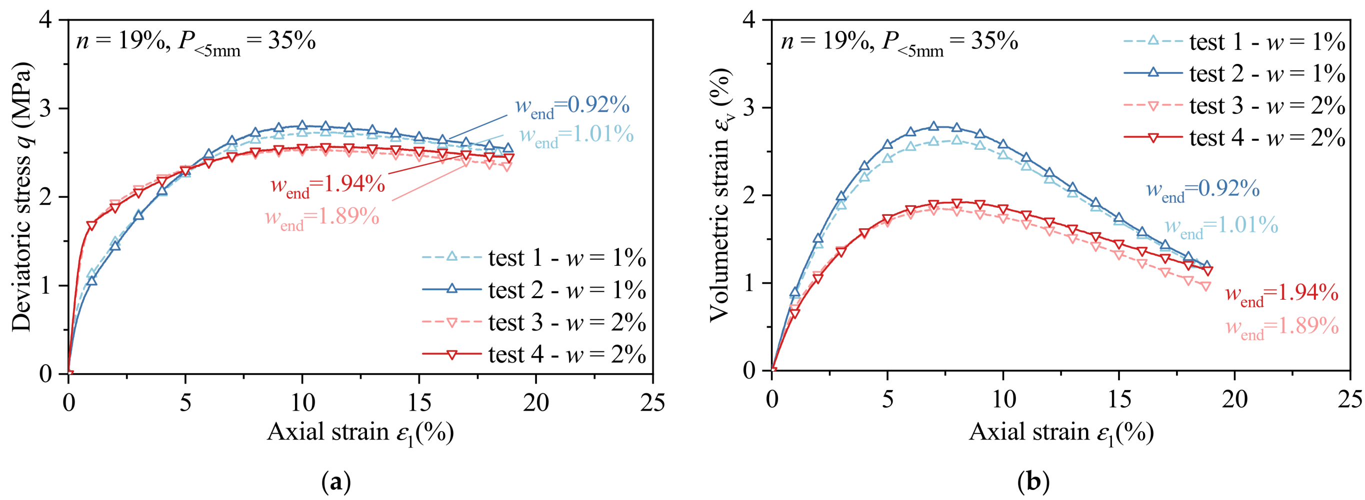

Figure 7. Verification of test repeatability for unsaturated rockfill specimens at σ_3 = 0.6 MPa: (**a**) deviatoric stress versus axial strain; (**b**) volumetric strain versus axial strain.

3. Test Results and Discussion

3.1. Stress–Strain Behaviour

Figure 8 shows the deviatoric stress–axial strain and volumetric strain–axial strain curves of unsaturated rockfill specimens (n = 19%; $P_{<5mm}$ = 35%) prepared at different moulding moisture contents under different confining pressures. In this study, positive volumetric strain denotes compression, whereas negative volumetric strain denotes dilation. The mechanical properties of rockfill material with different moisture contents are summarised in Table 3. Overall, specimens prepared at different moulding moisture contents exhibit the typical nonlinear stress–strain responses of granular materials. At lower confining pressures, the deviatoric stress increases rapidly with axial strain and reaches a peak, then shows varying degrees of softening over a large strain range, and finally tends to stabilise. As the confining pressure increases, both the peak deviatoric stress and maximum volumetric strain increase markedly, while stress softening and dilation become progressively less pronounced. Taking the specimen with w = 0% as an example, under σ_3 = 0.2 MPa, the deviatoric stress reaches its peak at ε_1 approximately 5% and then decreases noticeably. Under σ_3 = 2.5 MPa, the peak stress occurs later, at approximately ε_1 = 10%, and the post-peak reduction becomes much smaller. This behaviour is consistent with the typical response of rockfill materials under conventional triaxial compression [1].

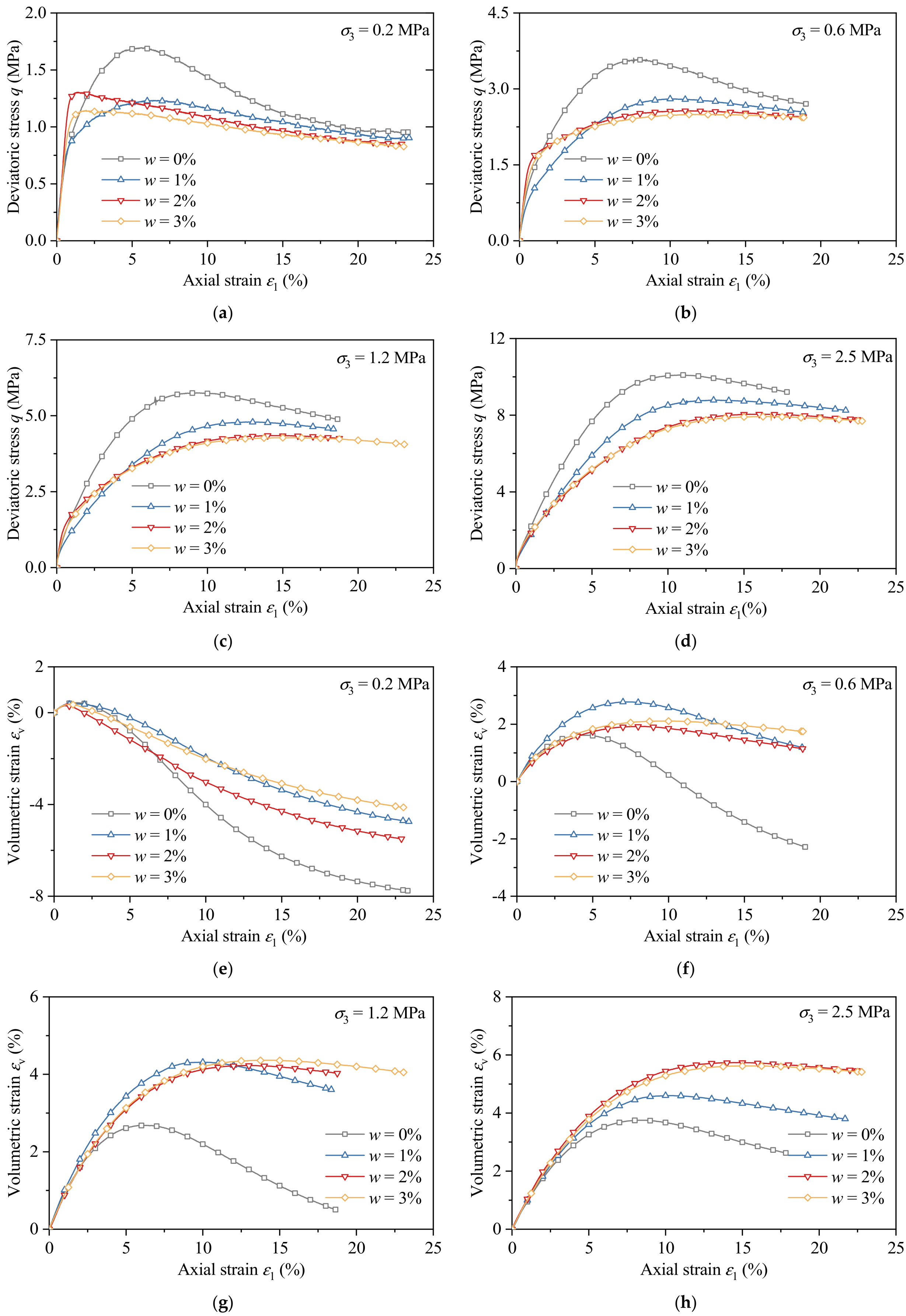

Figure 8. Results of triaxial shear tests under different moisture contents (n = 19%; $P_{<5\text{mm}}$ = 35%): (**a**–**d**) deviatoric stress versus axial strain and (**e**–**h**) volumetric strain versus axial strain.

Table 3. Test results on mechanical properties of rockfill material with different moisture contents.

Moisture Content (%)	σ_3 (MPA)	ε_{1max} (%)	ε_{vmax} (%)	q_{max} (MPA)	ϕ_p (°)
0	0.2	5.69	0.44	1.69	54.01
	0.6	8.00	1.62	3.57	48.47
	1.2	9.30	2.68	5.75	44.88
	2.5	10.87	3.75	10.1	41.99
1	0.2	6.65	0.39	1.23	49.02
	0.6	10.24	2.78	2.80	44.44
	1.2	12.71	4.31	4.80	41.80
	2.5	13.20	4.60	8.79	39.60
2	0.2	1.43	0.32	1.30	49.93
	0.6	10.88	1.92	2.57	42.98
	1.2	14.29	4.22	4.35	40.13
	2.5	16.22	5.74	8.05	38.10
3	0.2	1.96	0.36	1.14	47.82
	0.6	12.08	2.11	2.498	42.49
	1.2	15.35	4.36	4.28	39.85
	2.5	16.58	5.62	7.94	37.84

At a given confining pressure, the dry specimen (w = 0%) generally shows the highest peak deviatoric stress and the most pronounced post-peak softening. In contrast, specimens prepared with added water exhibit different degrees of peak-strength reduction, and the stress–strain curves become more gradual than those of the dry specimen. Previous studies have generally reported a gradual decrease in peak strength with increasing moisture content or decreasing suction. In the present tests, however, the peak strength at low confining pressure (σ_3 = 0.2 MPa) does not decrease monotonically with increasing moulding moisture content. When the moulding moisture content increases to w = 1%, the peak deviatoric stress decreases by 27% compared with that of the dry specimen. The peak deviatoric stress of the specimen with w = 2% is slightly higher than that of the specimen with w = 1%, although its post-peak softening is more pronounced. When the confining pressure increases to 0.6 MPa or above, the peak strength decreases monotonically with increasing moisture content.

Further comparison of the stress–strain curves at different moulding moisture contents shows that the curve for the specimen with w = 1% remains below that of the dry specimen throughout the loading process, indicating that even a small amount of water is sufficient to weaken both stiffness and strength. This is generally attributed to the reduction in interparticle friction with increasing moisture content and the decrease in apparent cohesion associated with lower matric suction. Because coarse-grained soils have large interparticle pores and relatively low suction, the behaviour observed in this study is mainly attributed to lubrication. As the moisture content further increases to 2% and 3%, the slope of the stress–strain curve in the initial axial strain range (<2%) increases markedly, and the initial modulus increases. The initial rising part of the curve may even lie above that of the dry specimen. This indicates that the moulding moisture content within this range improves the deformation resistance of the specimen during the early loading stage. Qiu et al. [38] also observed a similar increase in the elastic modulus with increasing moisture content in a study on the dynamic response of coarse-grained soils in different moisture states. However, this moisture-induced enhancement is limited to the initial axial strain range. With continued axial strain development, the stress–strain curves of the unsaturated rockfill gradually shift downward in the medium- and large-strain stages as moisture content increases. In other words, increasing the moulding moisture content mainly changes the early stiffness characteristics of the specimen, while it more readily causes a reduction in load-carrying capacity during subsequent shearing. Confining pressure also has a clear influence on the moulding moisture content effect. With increasing confining pressure, the modulus enhancement effect gradually weakens and nearly disappears when the confining pressure reaches 2.5 MPa.

Figure 8 also shows the volumetric strain–axial strain relationships of unsaturated rockfill specimens prepared at different moulding moisture contents. Overall, the dry specimens show more pronounced dilation. As the moulding moisture content increases, dilation is gradually suppressed, and volumetric compression increases. This behaviour is similar to the results of suction-controlled unsaturated tests [11,22,23]. It is worth noting that under low confining pressures (0.2–1.2 MPa), the difference in volumetric deformation among unsaturated specimens with different moisture contents is relatively small. The peak volumetric strain of the specimen with w = 1% is slightly larger than that of the specimens with w = 2% and w = 3%. A small amount of water mainly reduces interparticle friction, whereas a further increase in moisture content increases capillary forces between particles and may reduce compressibility to some extent. When the confining pressure increases to 2.5 MPa, the volumetric compression of the specimens with w = 2% and w = 3% increases sharply and becomes much higher than that of the dry specimen and the specimen with w = 1%. This difference may be related to different degrees of particle breakage.

3.2. Peak Friction Angle of Unsaturated Rockfill

Figure 9 presents the stress–strain curves under different confining pressures at w = 0%. It can be seen that the peak deviatoric stress increases continuously with increasing confining pressure. For a more direct comparison, the peak friction angle is calculated using the following formula:

$$\sin\phi_p = \frac{q_{\max}}{q_{\max} + 2\sigma_3} \tag{1}$$

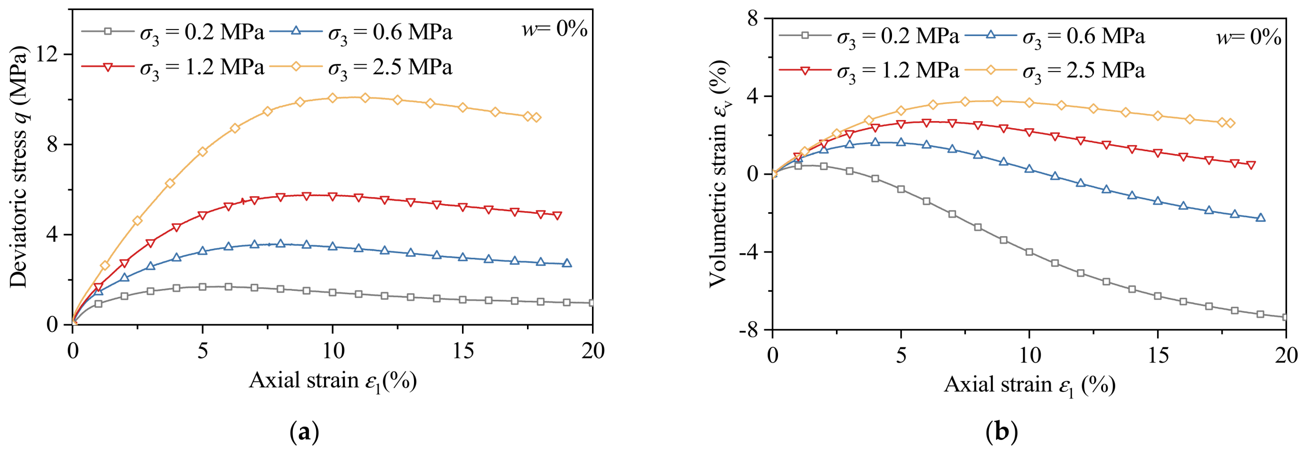

Figure 9. Results of triaxial shear tests under different confining pressures (n = 19%; $P_{<5mm}$ = 35%): (**a**) deviatoric stress versus axial strain and (**b**) volumetric strain versus axial strain.

Figure 10 shows the variation in the peak friction angle for specimens prepared at different moulding moisture contents.

Overall, under different confining pressures, the peak friction angle decreases with increasing moulding moisture content. Compared with the dry specimen, when the moulding moisture content increases from 0% to 1%, the ϕ_p of all specimen groups decreases markedly, indicating that adding a small amount of water can markedly reduce the shear strength of unsaturated rockfill. When the moisture content further increases to 2% and 3%, the variation in the peak friction angle becomes more gradual. At the same moulding moisture content, the peak friction angle decreases continuously as confining pressure increases; this may be due to increased particle breakage and a weakening of the interparticle bonds [39,40].

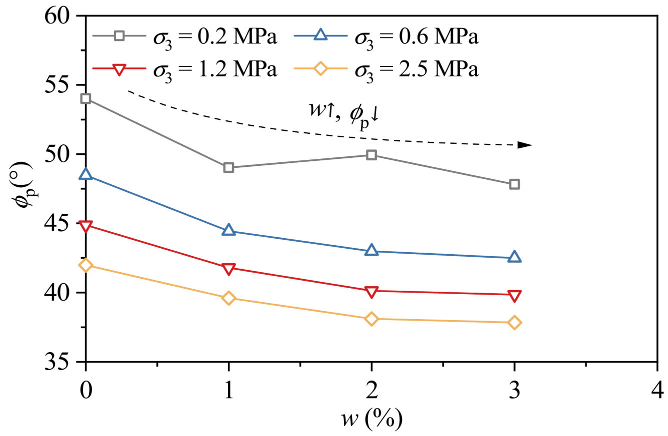

Figure 10. Effect of moulding moisture content on peak friction angle under different confining pressures.

Although a slight fluctuation in peak strength is observed at low confining pressure for the specimen with w = 2%, it remains lower than that of the dry specimen. Figure 11 shows the normalised attenuation of ϕ_p with moisture content, using the ϕ_p of the dry specimen as the reference ($R_w = \phi_{p,w=i\%}/\phi_{p,w=0\%}$). The peak strength is most sensitive to initial addition of moisture. The most pronounced strength reduction occurs when the moisture content increases from 0% to 1%. As the moulding moisture content continues to increase, the strength reduction becomes more moderate, and the weakening coefficient stabilises at approximately 0.87–0.91. The degree of peak strength reduction also varies with the confining pressure. As the confining pressure increases, the magnitude of strength attenuation gradually decreases.

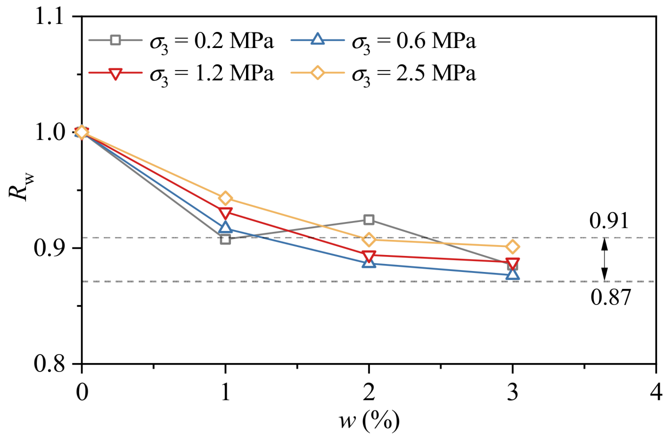

Figure 11. Evolution of the weakening coefficient with moisture content under different confining pressures.

3.3. Particle Breakage After Tests

For quantitative analysis, the post-test material was divided into four size groups after sieving: 20–60 mm, 10–20 mm, 5–10 mm, and <5 mm. Figure 12 shows the contents of these particle groups for unsaturated specimens prepared at different moulding moisture contents after drained shearing. The initial content represents the gradation before shearing. The results show that increasing confining pressure strongly promotes the breakage of coarse particles and the progressive generation of fine particles. As the confining pressure increases from 0.2 MPa to 2.5 MPa, the content of the 20–60 mm coarse-particle group continuously decreases, whereas the content of particles smaller than 5 mm increases continuously. In contrast, changes in the intermediate groups of 10–20 mm and 5–10 mm are less pronounced. This is because these groups may both be generated by the breakage of larger particles and further break into smaller particles during continued shearing [41]. Regarding the effect of moulding moisture content on particle breakage, under low confining pressures (0.2 and 0.6 MPa), the post-shearing gradations of specimens with different moulding moisture contents are generally similar. Under medium and high confining pressures, the differences among specimens become more pronounced. Overall, with increasing moulding moisture content, the 20–60 mm group further decreases, and the <5 mm group further increases, indicating that specimens with higher moulding moisture contents are more prone to particle breakage under higher confining pressures.

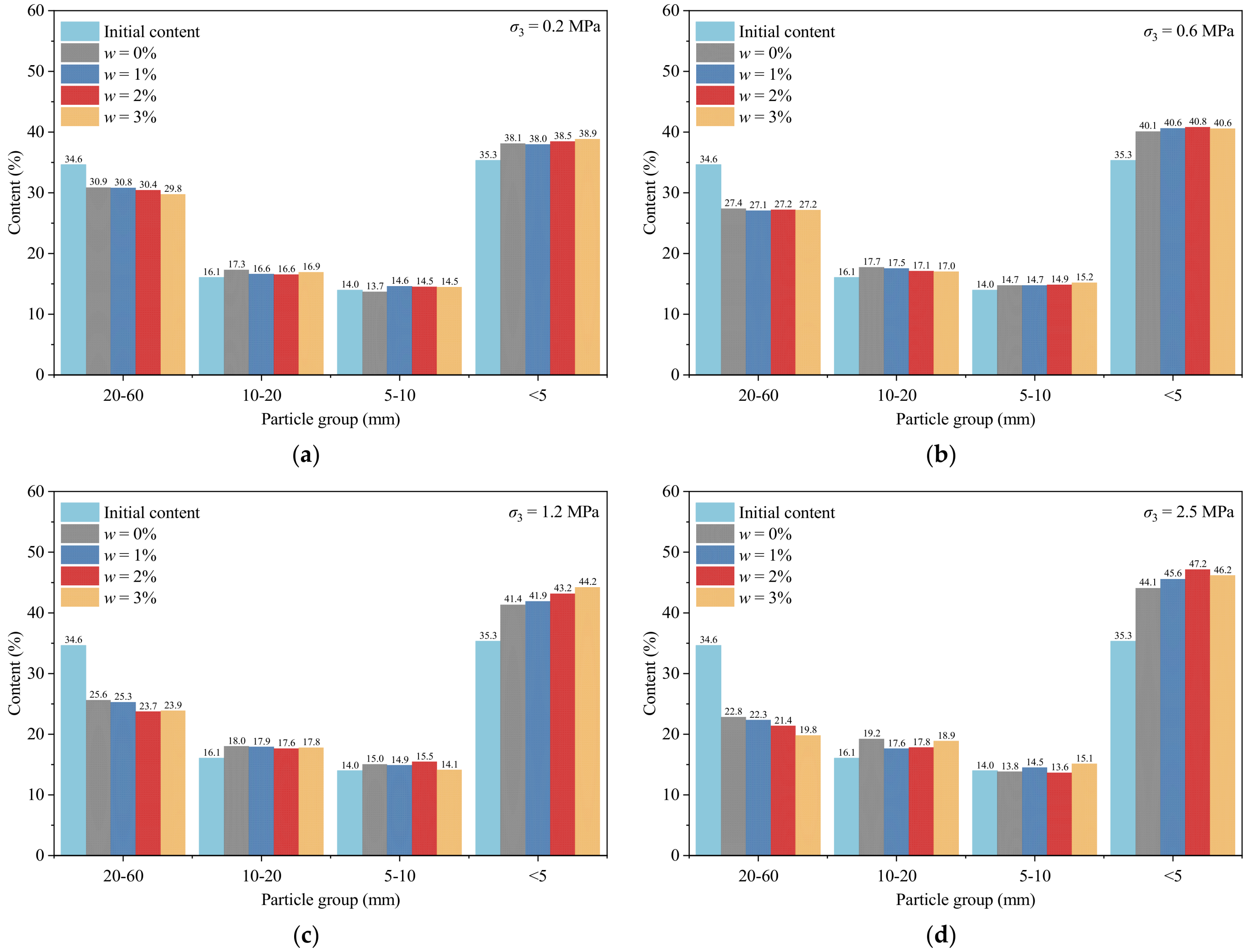

Figure 12. The variation in contents of particle groups for specimens with different moisture contents: (**a**) 0.2 MPa, (**b**) 0.6 MPa, (**c**) 1.2 MPa, and (**d**) 2.5 MPa.

3.4. Effect of Fines Content on the Moulding Moisture Content Effect

Figure 13 shows the deviatoric stress–axial strain and volumetric strain–axial strain relationships for specimens with an initial porosity of n = 19%, a fines content of $P_{<5mm}$ = 19%, and a confining pressure of σ_3 = 0.6 MPa. This test series is compared with the reference condition (n = 19%; $P_{<5mm}$ = 35%) to investigate the influence of fines content on the moulding moisture content effect. The deviatoric stress–axial strain curves show that the dry specimen (w = 0%) still has the highest peak deviatoric stress and pronounced post-peak softening. In contrast, the peak deviatoric stresses of the unsaturated specimens prepared with moisture are all lower than that of the dry specimen. Notably, after reducing the fines content, the differences among specimens with different moulding moisture contents become more pronounced in the early stage of shearing. With only 1% moisture added during preparation, the specimen shows a faster increase in deviatoric stress at small strains, and its initial loading segment nearly overlaps with that of the dry specimen. However, as axial strain increases, its strength growth gradually slows and becomes lower than that of the dry specimen in the medium- and large-strain stages. In contrast, for the specimens with $P_{<5mm}$ = 35%, the curve for the specimen with w = 1% remains below that of the dry specimen. The volumetric strain curves follow the same trend as the reference condition $P_{<5mm}$ = 35%. The dry specimen shows the most pronounced dilation, whereas moisture addition suppresses dilation to different degrees and makes the overall volumetric deformation more compressive. These results indicate that lowering the fines content makes the rockfill more sensitive to moulding moisture content, especially in terms of the non-monotonic variation in initial stiffness. The coupled influence of fines and moisture content has also been reported for coarse–fine soil mixtures. Duong et al. [13] showed that the effects of water content and fines content on the resilient modulus are closely linked, while Su et al. [14] demonstrated that water content and coarse-particle proportion jointly influence permanent deformation. These findings support the present observation that changes in fines content can modify the sensitivity of coarse-grained materials to moisture variation.

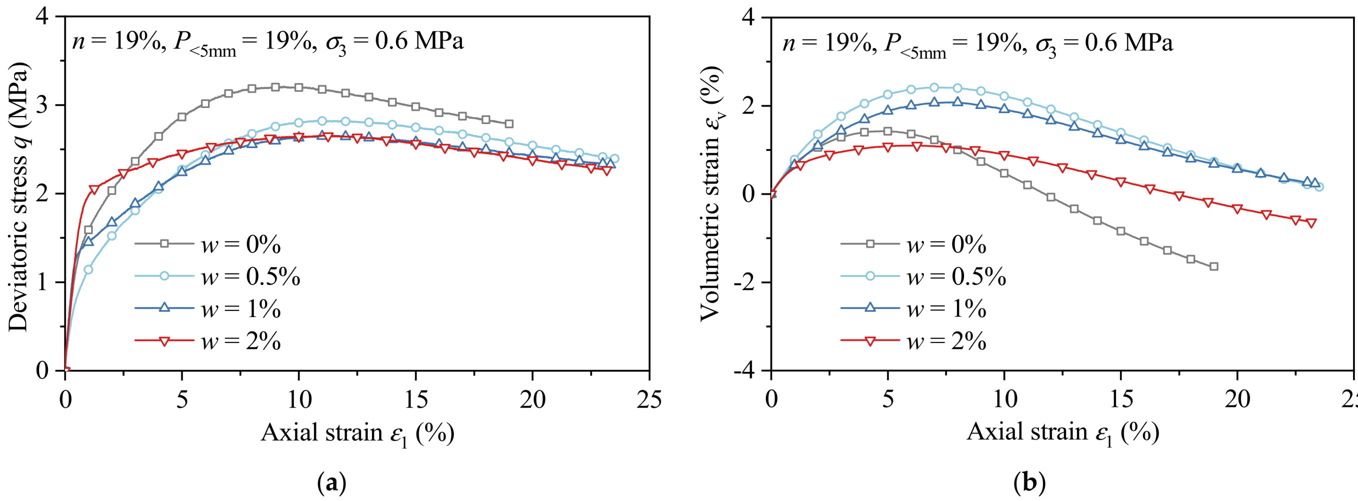

Figure 13. Effect of fines content on the moisture content response at n = 19% and $P_{<5mm}$ = 19%: (**a**) deviatoric stress versus axial strain and (**b**) volumetric strain versus axial strain.

3.5. Effect of Initial Porosity on the Moulding Moisture Content Effect

Figure 14 shows the deviatoric stress–axial strain and volumetric strain–axial strain relationships for the condition with n = 21%, $P_{<5mm}$ = 35%, and σ_3 = 0.6 MPa. This test series is compared with the reference condition (n = 19%; $P_{<5mm}$ = 35%) to analyse the influence of initial density on the moulding moisture content effect. The deviatoric stress–axial strain curves show that when the initial porosity increases from 19% to 21%, the overall deviatoric stress level decreases markedly. This indicates that the reduced compactness of the initial skeleton weakens interparticle interlocking, thereby reducing the strength differences among specimens with different moisture contents. In addition, the differences in the initial loading segment among specimens with different moulding moisture contents become smaller. Although the initial modulus enhancement can still be observed under certain moulding moisture contents, its magnitude is much smaller than that observed for n = 19%. The volumetric strain curves further show that specimens with higher porosity exhibit greater overall compression and weaker dilation during shearing, and the volumetric strain curves of the specimens with 1% and 2% moulding moisture contents are nearly identical. These results indicate that increasing initial porosity weakens the overall influence of moulding moisture content on peak strength and initial stiffness, although the non-monotonic modulus enhancement feature is still retained.

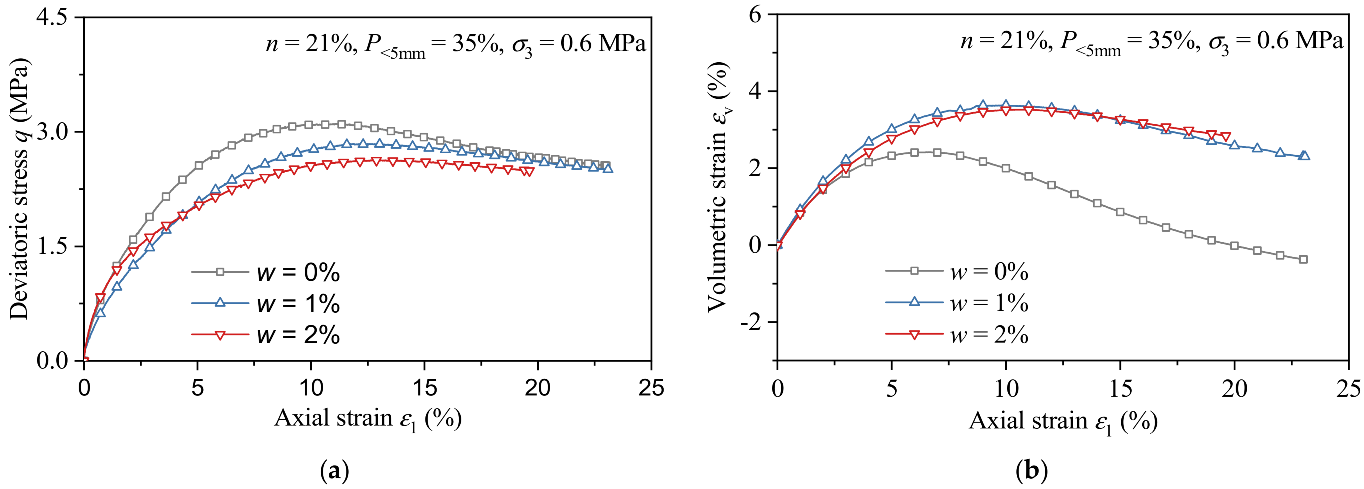

Figure 14. Effect of initial porosity on the moisture content response at n = 21% and $P_{<5mm}$ = 35%: (**a**) deviatoric stress versus axial strain; (**b**) volumetric strain versus axial strain.

3.6. Mechanistic Interpretation and Discussion

Previous studies on unsaturated soils have commonly been based on the suction framework, in which soil strength and stiffness generally decrease monotonically with increasing moisture content or decreasing suction [22,23]. However, the present test results show that the effect of moulding moisture content on the mechanical response of rockfill material does not follow this simple trend, especially for the initial modulus, which shows a clear non-monotonic feature. Figure 15 shows the deviatoric stress–axial strain and volumetric strain–axial strain curves of specimens prepared at different moulding moisture contents after saturation. Even after all specimens experience saturation, the deviatoric stress–axial strain and volumetric strain–axial strain curves still differ markedly among specimens prepared at different moulding moisture contents. Because saturation largely eliminates matric suction within the specimens, the mechanical responses of all groups would be expected to become similar after saturation if the moulding moisture content effect were mainly caused by suction differences during shearing. The observed differences indicate that moulding moisture content may change particle rearrangement, fines distribution, contact state, and initial damage during compaction, and that these initial fabric differences are not fully removed by subsequent saturation. Therefore, matric suction is not the only controlling factor for the effect of moulding moisture content on the mechanical properties of unsaturated rockfill material. Initial fabric differences formed during specimen preparation may be a more fundamental reason for the different mechanical responses.

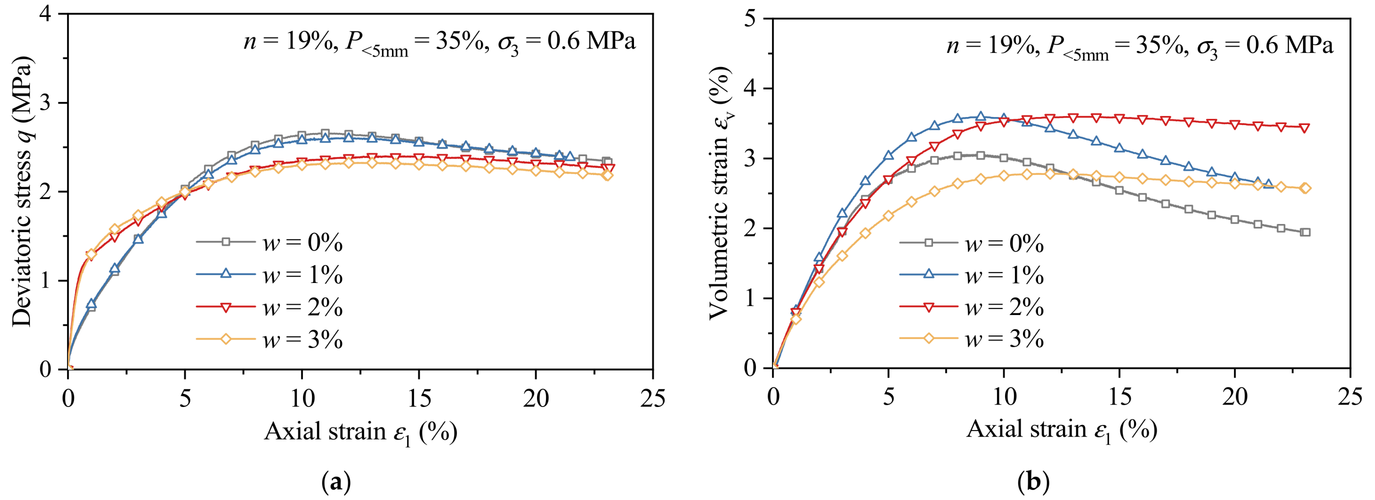

Figure 15. Mechanical responses after saturation of specimens prepared at different moisture contents: (**a**) deviatoric stress versus axial strain; (**b**) volumetric strain versus axial strain.

To further characterise the difference caused by the initial structure, the secant modulus within the small-strain range, $E_{0.5\%}$, was used as the initial modulus parameter. Figure 16 shows the variation in the normalised initial modulus, $E_{0.5\%}/E_{0.5\%,w=0\%}$, with moisture content. The results show that, at different fines contents and porosities, the initial modulus consistently exhibited a non-monotonic variation with moulding moisture content. It first decreased and then increased. Under the reference condition with n = 19% and $P_{<5mm}$ = 35%, the initial modulus decreased markedly when the moulding moisture content increased from 0% to 1%. When the moisture content further increased to 2%, the initial modulus recovered significantly and exceeded that of the dry specimen. This result indicates that the influence of moulding moisture content on the initial stiffness of rockfill materials is not a monotonic weakening process but involves a transition from "lubrication weakening" to "fabric stabilisation". Chen and Yang [27] showed that the initial stiffness of granular mixtures is sensitive to the contact fabric formed during specimen preparation. When a small amount of moisture is added, moisture produces a lubrication effect at particle contacts, reducing interparticle friction and local interlocking strength. The specimen, therefore, more readily undergoes contact sliding and structural adjustment during the early stage of shearing, which reduces the initial stiffness. As the moulding moisture content further increases, capillary effects between particles become stronger, and greater compaction effort is required during specimen preparation. This may promote a more coordinated and stable particle skeleton, leading to the recovery of the initial modulus and even values higher than that of the dry specimen. Porosity and fines content clearly regulate this process. After porosity increases, the variation in the initial modulus with moisture content becomes much weaker, indicating that the smaller number of particle contacts in a looser skeleton makes it difficult for local moisture effects to significantly change the overall force chain structure. In contrast, after the fines content decreases, the initial modulus becomes more sensitive to moisture content, indicating that when the coarse-particle skeleton dominates, moisture affects the contact state more directly. The lubrication, adsorption, and local capillary effects at key contacts are more easily reflected in the macroscopic mechanical response.

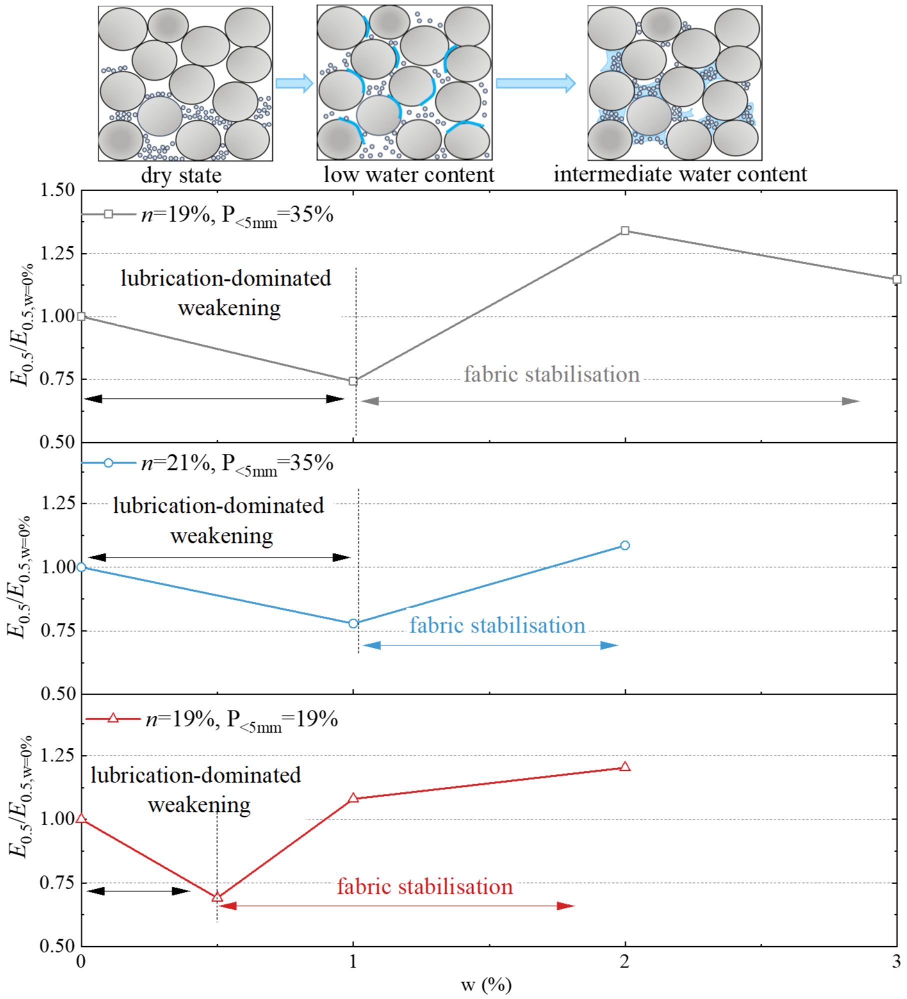

Figure 16. Influence of moisture content on the initial secant modulus under different initial conditions.

The effect of moulding moisture content on the mechanical properties of unsaturated rockfill identified in this study indicates that, for earth-rock dams and high-fill projects, moisture content should not be regarded only as a factor affecting compaction efficiency. It should also be treated as an important control parameter for the initial mechanical properties and deformation response of rockfill materials. This is particularly important for rockfill materials with a coarse-particle skeleton and relatively low fines content, for which moisture variation may cause pronounced differences in stiffness and deformation. Therefore, moisture content control during construction should be strengthened. This study also has some limitations. First, the observed trends were obtained within limited ranges of porosity and fines content and should be further verified under more gradation conditions and a wider moisture content range. Second, suction was not measured due to limitations of the test conditions. Future studies should combine microscopic observations, suction measurements, and the discrete element method to further reveal the mechanism by which moulding moisture content affects rockfill behaviour.

4. Conclusions

In this study, a series of large-scale triaxial compression tests was conducted on unsaturated rockfill materials to investigate the effect of moulding moisture content on their mechanical properties. The main conclusions are summarised as follows.

An increase in the moulding moisture content significantly reduced the peak deviatoric stress and peak friction angle of unsaturated rockfill. The most pronounced strength degradation occurred when the moisture content increased from 0% to 1%, after which the strength weakening coefficient stabilised between 0.87 and 0.91.

Increasing the moulding moisture content weakened the dilation of unsaturated rockfill specimens. With increasing confining pressure, specimens prepared at higher moulding moisture contents showed more particle breakage, a further decrease in the coarse-particle group (20–60 mm), a further increase in the fine-particle group (<5 mm), and more pronounced volumetric compression.

The initial modulus of unsaturated rockfill did not decrease monotonically with increasing moulding moisture content. At lower moisture contents, such as 1%, the lubrication effect of moisture dominated and reduced interparticle contact friction, leading to a decrease in initial stiffness. When the moisture content further increased, such as to 2% or higher, a stronger capillary effect may have required greater compaction effort and promoted a more coordinated and stable particle skeleton, causing the initial modulus to recover and even exceed that of the dry specimen.

The moulding moisture content effect strongly depended on the initial physical state of the material. Reducing the fines content made the macroscopic mechanical response more sensitive to moisture variation. In contrast, increasing initial porosity weakened interparticle interlocking, reduced the overall deviatoric stress level, and thereby weakened the influence of moulding moisture content.

After complete saturation, the stress–strain and volumetric strain curves of specimens prepared at different moulding moisture contents still show clear differences. This indicates that moisture action during specimen preparation may form irreversible differences in initial fabric. Therefore, in earth-rock dam and high-fill engineering practice, moulding moisture content should not be treated only as a construction index related to compaction efficiency but should be properly controlled as a key parameter governing the initial mechanical properties of coarse-grained soils.

Author Contributions: G.C.: methodology, investigation, data curation, visualisation, and writing—original draft. H.Y.: investigation, data curation, validation, and visualisation. D.Z.: supervision, funding acquisition, and writing—review and editing. F.N.: conceptualisation, methodology, supervision, project administration, funding acquisition, and writing—review and editing. J.L.: resources, methodology, supervision, and writing—review and editing. C.Z.: resources, investigation, data curation, and validation. X.Z.: resources, investigation, data curation, and validation. All authors have read and agreed to the published version of the manuscript.

Funding: This research was supported by the National Natural Science Foundation of China (Grant Nos. 52479119, 52350393 and U23B20149) and the Fundamental Research Funds for the Central Universities (DUTZD25101).

Institutional Review Board Statement: Not applicable.

Informed Consent Statement: Not applicable.

Data Availability Statement: The original contributions presented in this study are included in the article. Further inquiries can be directed to the corresponding author.

Conflicts of Interest: Authors Huizong Yan and Xinyuan Zhang were employed by the company POWERCHINA Kunming Engineering Corporation, Limited. All authors declare that the research was conducted in the absence of any commercial or financial relationships that could be construed as a potential conflict of interest.

References

1. Varadarajan, A.; Sharma, K.G.; Venkatachalam, K.; Gupta, A.K. Testing and modeling two rockfill materials. *J. Geotech. Geoenviron. Eng.* **2003**, *129*, 206–218. [CrossRef]
2. Xiao, Y.; Liu, H.; Chen, Y.; Jiang, J. Strength and deformation of rockfill material based on large-scale triaxial compression tests. I: Influences of density and pressure. *J. Geotech. Geoenviron. Eng.* **2014**, *140*, 4014070. [CrossRef]
3. Xiao, Y.; Liu, H.L.; Chen, Y.M.; Jiang, J.S. Strength and deformation of rockfill material based on large-scale triaxial compression tests. II: Influence of particle breakage. *J. Geotech. Geoenviron. Eng.* **2014**, *140*, 4014071. [CrossRef]
4. Kermani, M.; Konrad, J.M.R.E.; Smith, M. An empirical method for predicting post-construction settlement of concrete face rockfill dams. *Can. Geotech. J.* **2017**, *54*, 755–767. [CrossRef]
5. Ning, F.; Liu, J.; Kong, X.; Zou, D. Critical state and grading evolution of rockfill material under different triaxial compression tests. *Int. J. Geomech.* **2020**, *20*, 4019154. [CrossRef]
6. Ning, F.W.; Liu, J.M.; Zou, D.G.; Kong, X.J.; Cui, G.Y. Super-large-scale triaxial tests to study the effects of particle size on the monotonic stress--strain response of rockfill materials. *Acta Geotech.* **2025**, *20*, 1847–1858. [CrossRef]
7. Oldecop, L.A.; Alonso, E.E. A model for rockfill compressibility. *Géotechnique* **2001**, *51*, 127–139. [CrossRef]
8. Wu, Y.; Yin, Y.; Zhang, B.; Sun, X.; Yu, Y. Unsaturated wetting deformation characteristics of a granite rockfill under rainfall conditions. *Can. Geotech. J.* **2022**, *59*, 1774–1792. [CrossRef]
9. Cetin, H.; Laman, M.; Ertunc, A. Settlement and slaking problems in the world's fourth largest rock-fill dam, the Ataturk Dam in Turkey. *Eng. Geol.* **2000**, *56*, 225–242. [CrossRef]
10. Hunter, G.; Fell, R. Rockfill modulus and settlement of concrete face rockfill dams. *J. Geotech. Geoenviron. Eng.* **2003**, *129*, 909–917. [CrossRef]
11. Ishikawa, T.; Zhang, Y.; Tokoro, T.; Miura, S. Medium-size triaxial apparatus for unsaturated granular subbase course materials. *Soils Found.* **2014**, *54*, 67–80. [CrossRef]
12. Zhao, H.F.; Zhang, L.M. Effect of coarse content on shear behavior of unsaturated coarse granular soils. *Can. Geotech. J.* **2014**, *51*, 1371–1383. [CrossRef]
13. Duong, T.V.; Cui, Y.J.; Tang, A.M.; Dupla, J.C.; Canou, J.; Calon, N.; Robinet, A. Effects of water and fines contents on the resilient modulus of the interlayer soil of railway substructure. *Acta Geotech.* **2015**, *11*, 51–59. [CrossRef]
14. Su, Y.; Cui, Y.J.; Dupla, J.C.; Canou, J. Effect of water content on permanent deformation of fine/coarse soil mixtures with varying coarse grain contents and subjected to multi-stage cyclic loading. *Acta Geotech.* **2022**, *17*, 3259–3268. [CrossRef]
15. Indraratna, B.; Wijewardena, L.; Balasubramaniam, A.S. Large-scale triaxial testing of grey wacke rockfill. *Géotechnique* **1993**, *43*, 37–51. [CrossRef]
16. Shi, X.S.; Liu, K.; Yin, J. Effect of initial density, particle shape, and confining stress on the critical state behavior of weathered gap-graded granular soils. *J. Geotech. Geoenviron. Eng.* **2021**, *147*, 4020160. [CrossRef]
17. Guo, W.L.; Chen, G. Particle breakage and gradation evolution of rockfill materials during triaxial shearing based on the breakage energy. *Acta Geotech.* **2022**, *17*, 5351–5358. [CrossRef]
18. Cui, G.; Zou, D.; Ning, F.; Liu, J.; Li, D.; Tian, S.; Han, M. Coupled effect of particle shape and particle breakage on strength--dilatancy and critical state behaviors of coarse-grained soils. *Acta Geotech.* **2026**, *21*, 2099–2114. [CrossRef]
19. Mao, H.; Shen, C.; Liu, S.; Wang, L.; Fu, Z. Insight into the crushing strength of rockfill grains at different temperature and relative humidity conditions. *Rock Mech. Rock Eng.* **2023**, *56*, 6529–6543. [CrossRef]
20. Jia, Y.; Xu, B.; Desai, C.S.; Chi, S.; Xiang, B. Rockfill particle breakage generated by wetting deformation under the complex stress path. *Int. J. Geomech.* **2020**, *20*, 4020166. [CrossRef]
21. Cui, G.Y.; Liu, J.M.; Ning, F.W.; Zou, D.G.; Kong, X.J.; Fu, Y.K. Experimental study on wetting deformation of rockfill materials under different stress paths. *J. Geotech. Geoenviron. Eng.* **2025**, *151*, 4025066. [CrossRef]
22. Vanapalli, S.K.; Fredlund, D.G.; Pufahl, D.E.; Clifton, A.W. Model for the prediction of shear strength with respect to soil suction. *Can. Geotech. J.* **1996**, *33*, 379–392. [CrossRef]
23. Maleki, M.; Bayat, M. Experimental evaluation of mechanical behavior of unsaturated silty sand under constant water content condition. *Eng. Geol.* **2012**, *141*, 45–56. [CrossRef]
24. Zhou, A.; Huang, R.; Sheng, D. Capillary water retention curve and shear strength of unsaturated soils. *Can. Geotech. J.* **2016**, *53*, 974–987. [CrossRef]
25. Acheampong, L.; Bryson, L.S. Development of a scaling function to estimate unsaturated mechanical soil behavior from a soil-water characteristic curve. *Can. Geotech. J.* **2024**, *62*, 1–20. [CrossRef]
26. Oualmakran, M.; Mercatoris, B.; François, B. Pore-size distribution of a compacted silty soil after compaction, saturation, and loading. *Can. Geotech. J.* **2016**, *53*, 1902–1909. [CrossRef]
27. Chen, Y.; Yang, J. Small-strain shear modulus of silty sands: The role of sample preparation method. *Géotechnique* **2024**, *74*, 367–382. [CrossRef]

28. Mousavi, M.; Disfani, M.M.; Black, J.R.; Mehdizadeh, A. Impact of sample preparation on erosion characteristics and subsequent mechanical behaviour of gap-graded soils: An imaging-based analysis. *Can. Geotech. J.* **2025**, *62*, 1–19. [CrossRef]
29. Delage, P.; Audiguier, M.; Cui, Y.J.; Howat, M.D. Microstructure of a compacted silt. *Can. Geotech. J.* **1996**, *33*, 150–158. [CrossRef]
30. De Magistris, F.S.; Tatsuoka, F. Effects of moulding water content on the stress-strain behaviour of a compacted silty sand. *Soils Found.* **2004**, *44*, 85–101. [CrossRef] [PubMed]
31. Zhang, T.W.; Cui, Y.J.; Lamas-Lopez, F.; Calon, N.; D'aGuiar, S.C. Compacted soil behaviour through changes of density, suction, and stiffness of soils with remoulding water content. *Can. Geotech. J.* **2018**, *55*, 182–190. [CrossRef]
32. Ng, C.W.W.; Peprah-Manu, D. Influence of aggregate structure on the compressibility of an unsaturated compacted silty sand. *Eng. Geol.* **2023**, *314*, 107007. [CrossRef]
33. Dai, B.L.; Zhou, C.; Mu, Q.Y.; Peng, J.B. Evolution of structure and anisotropic shear stiffness of compacted loess during compression. *Can. Geotech. J.* **2025**, *62*, 1–13. [CrossRef]
34. *ASTM D7012-23*; Standard Test Methods for Compressive Strength and Elastic Moduli of Intact Rock Core Specimens Under Varying States of Stress and Temperatures. ASTM International: West Conshohocken, PA, USA, 2023.
35. *GB/T 50123-2019*; Standard for Geotechnical Testing Method. China PLanning Press: Beijing, China, 2019.
36. Xie, K.; Chen, X.B.; Li, T.F.; Deng, Z.X.; Yao, J.K.; Tang, L.B. A framework for determining the optimal moisture content of high-speed railway-graded aggregate materials based on the lab vibration compaction method. *Constr. Build. Mater.* **2023**, *392*, 131764. [CrossRef]
37. *ASTM D7181-20*; Standard Test Method for Consolidated Drained Triaxial Compression Test for Soils. ASTM International: West Conshohocken, PA, USA, 2020.
38. Qiu, M.; Luo, X.; Tang, L.; Tian, S.; Sun, Y.; Bhattacharya, S.; Ling, X. Experimental investigation on dynamic characteristics of gravel soil filler for railway subgrade affected by varying initial moisture content. *Transp. Geotech.* **2026**, *59*, 101907. [CrossRef]
39. Wu, Z.Y.; Chen, J.K. Pressure-dependent variability in shear strength of a blasting-quarried granite rockfill material. *Soils Found.* **2019**, *59*, 2299–2310. [CrossRef]
40. Indraratna, B.; Ionescu, D.; Christie, H.D. Shear behavior of railway ballast based on large-scale triaxial tests. *J. Geotech. Geoenviron. Eng.* **1998**, *124*, 439–449. [CrossRef]
41. Yu, J.; Shen, C.; Liu, S.; Cheng, Y.P. Exploration of the survival probability and shape evolution of crushable particles during one-dimensional compression using dyed gypsum particles. *J. Geotech. Geoenviron. Eng.* **2020**, *146*, 4020121. [CrossRef]

Disclaimer/Publisher's Note: The statements, opinions and data contained in all publications are solely those of the individual author(s) and contributor(s) and not of MDPI and/or the editor(s). MDPI and/or the editor(s) disclaim responsibility for any injury to people or property resulting from any ideas, methods, instructions or products referred to in the content.